氧化石墨烯/聚合物基复合膜对水，氨水与二氯甲烷的渗透性

Ali Asghar Zomorodkia[1], Saeed Bazgir[2], Davood Zaarei[3], Mohsen Gorji[4], Mehdi Ardjmand[5]

(1. *Department of Chemical Engineering, Science and Research Branch, Islamic Azad University, Tehran, Postal code*: 1477893855, *Iran*;
2. *Department of Polymer Engineering, Science and Research Branch, Islamic Azad University, Tehran, Postal code*: 1477893855 *Iran*;
3. *Department of Polymer Engineering, South Tehran Branch, Islamic Azad University, Tehran, Postal code*: 1584743311, *Iran*;
4. *New Technologies Research Center (NTRC) Amirkabir University of Technology, Tehran, Postal code*: 159163 - 4311, *Iran*;
5. *Department of Chemical Engineering, South Tehran Branch, Islamic Azad University, Tehran, Postal code*: 1584743311, *Iran.*)

摘 要： 以氧化石墨烯(GO)、聚氨酯(PU)和亲水性聚 2-丙烯酰胺-2 -甲基丙烷磺酸(PAMPS)为原料，制备出无支撑的 PU 基复合膜和 PAMPS 基复合膜。研究氧化石墨烯聚合物基膜用于含极性材料废液如水、氨水、以及含非极性二氯甲烷和氨-二氯甲烷混合废液的渗透行为。采用不同表征方法如 X 射线衍射仪(XRD)、接触角、场发射扫描电子显微镜(FESEM)、红外光谱仪(FT-IR)和力学性能测试仪来评价所制复合膜的综合性能。采用 ASTM E96/96-M14 设备进行复合膜的渗透测试。结果表明，PAMPS 基复合膜因较高的亲水性，具有最佳的水和氨渗透性能，而 PU 基复合膜具有最佳的二氯甲烷渗透性，最差的水和氨的渗透性。

关键词： 聚氨酯；聚 2-丙烯酰胺-2 -甲基丙烷磺酸；氧化石墨烯；渗透性；疏水性；亲水性

中图分类号： TB33 **文献标识码：** A

通讯作者：Saeed Bazgir. E-mail：bazgir@ srbiau. ac. ir

Permeation of water, ammonia and dichloromethane through graphene oxide/polymeric matrix composite membranes

Ali Asghar Zomorodkia[1], Saeed Bazgir[2], Davood Zaarei[3], Mohsen Gorji[4], Mehdi Ardjmand[5]

(1. *Department of Chemical Engineering, Science and Research Branch, Islamic Azad University, Tehran, Postal code*: 1477893855, *Iran*;
2. *Department of Polymer Engineering, Science and Research Branch, Islamic Azad University, Tehran, Postal code*: 1477893855 *Iran*;
3. *Department of Polymer Engineering, South Tehran Branch, Islamic Azad University, Tehran, Postal code*: 1584743311, *Iran*;
4. *New Technologies Research Center (NTRC) Amirkabir University of Technology, Tehran, Postal code*: 159163-4311, *Iran*;
5. *Department of Chemical Engineering, South Tehran Branch, Islamic Azad University, Tehran, Postal code*: 1584743311, *Iran*)

Abstract: The permeation of polar molecules (water and ammonia), non-polar dichloromethane and a mixture of ammonia and dichloromethane through graphene oxide (GO)/polymer matrix composite membranes was investigated. Results indicated that a hydrophilic poly(2-acrylamido -2 -methyl propane sulfonic acid) (PAMPS) based membrane had the highest permeability for water and ammonia due to the high hydrophilicity of the polymer matrix while a hydrophobic polyurethane (PU)-based membrane had the best permeation performance for dichloromethane and the worst performance for water and ammonia. Adding the GO to PU or PAMPS polymers increases the negative charge due to the negatively charged nature of GO caused by its oxygen-containing functional groups, which increases the amounts of absorbed water and ammonia due to the positive charge of the hydrogen atoms in these two molecules.

Key words: PU; PAMPS; Graphene oxide; Permeability; Hydrophobic; Hydrophilic

Received date: 2020-02-02; *Revised date*: 2020-03-13

Corresponding author: Saeed Bazgir. E-mail: bazgir@ srbiau. ac. ir

1 Introduction

Todays, separation is an essential part of the processes in the chemical, petrochemical, biochemical, food and pharmaceutical industries. The goal of all these processes is enrichment, concentration, purification, and separation of each of the desired products from a mixture[1,2]. To this end, efficient separation processes are needed to obtain valuable products in the food and pharmaceutical industries to provide high quality and healthy water for various industries and communities, as well as removal and recy-

cling of toxic and microbial or valuable components from the industrial wastewater[2]. Filtration is one of the methods in which mass transfer operations are carried out within the initial phase using a barrier. The separator used for separation of the materials with a size above one micron is called the filter and the one used for separation of the substances with a size below one micron is called the membrane[3]. The membrane is an immiscible intermediate phase located between two adjacent phases that control the transfer of materials between the two phases by screening or controlling their relative transfer rates. A membrane acts as a barrier that selectively separates two phases against the transfer of different chemical species[2,3].

As the newest member of the graphite carbon family, graphene consists of fullerene as zero-dimensional nanoparticles, carbon nanotubes as one-dimensional nanoparticles, and graphite as a three-dimensional material. Graphene is a two-dimensional sheet of carbon atoms in a hexagonal configuration. The carbon atoms in graphene are bonded by the sp^2 hybrid. The discovery of the graphene has led to a great deal of research interest worldwide. However, like other newly discovered forms of carbon, such as fullerenes and carbon nanotubes, material availability is the speed-limiting factor in the process of evaluating graphene utilization. Graphene oxide (GO) has a large number of oxygenated functional groups such as hydroxyl, epoxy, and carboxyl at the surface and the edges[4]. These functional groups are good hydrophilic species and have good solubility in the water, making them a suitable and cost-effective solution for the preparation of GO-based membranes[5]. In addition, oxygenated functional groups make the GO nanoparticles fully recover and the GO functionalized composite membranes with desirable separation performance. Given these advantages as well as the high surface-to-volume ratio of GO nanofibers, GO-based membranes are widely developed and used in many areas of membrane separation such as gas separation and water purification[6-8].

In recent decades, inventions and papers (including research papers and reviews) have increasingly focused on the GO-based membranes[4]. The nanoparticles present in the membrane structures prevent the direct penetration of gas or vapors through the membrane and consciously increase the penetration path of the gases into the membrane. There are two main reasons for blocking gas or vapors in the GO-based polymer membranes including negative charge load and the porous passage path[9,10]. After the addition of the GO, due to its high volume and presence of oxygenated species, a small amount of negative charge would act as the barrier for permeation of the gases and vapors through the membranes[9, 10].

The important thing about two-dimensional fillers such as GO is that the two-dimensional GO structures are impermeable to most of the gases due to their negative surface charge and high surface-to-volume ratio. Three-dimensional polymer membranes combined with two-dimensional GO fillers can also act as a barrier against gases and vapors. Two-dimensional filler structures create a porous pathway for passage of the gases, which, as a result, increases the porosity in the polymeric sample and causes more surface area for the adsorption process, and therefore the time or gas transit time from the porous membrane increases and more gas absorption occurs by the GO[9,10].

Polyurethane (PU) is a hydrophobic three-dimensional polymer made from two basic precursors of polyol and isocyanate[11]. This polymer has been used as a very good material for water/oil separation, as it rarely allows the passage of water through the membrane due to its hydrophobic properties[12,13]. The addition of the GO to PU also increases its hydrophobicity and makes it a highly effective adsorbent or membrane in the liquid phase separation or air separation such as separation of N_2/CO_2. Adding the GO to PU makes the composite membrane highly selective to organic and non-hydrophilic substances such as oil, olefin, dichloromethane, DMF (Dimethylformamide), and many other non-polar organic materials[2,8,10,11]. Due to the hydrophobicity, the GO with a unique 2D structure and large specific surface area is a very suitable material for modification of the PU polymers. These polymers are superhydrophobic and have a high selectivity for separation of different oils and non-polar solvents (dichloromethane) from the water, therefore, the hydrophobicity would increase the permeability only in non-polar compounds such as dichloromethane, and it has the opposite effect in the polar solutions[14-17].

Several studies have been conducted on the permeability of the PU-GO membranes for water/oil separation, which show that this membrane is superhydrophobic and does not allow water pass through while the oil is easily crossed or absorbed[12,13]. Despite a lot of researches on the permeability of gas mixtures such as air, no research has been done in the field of polar vapors, such as water and ammonia[11].

Permeability of the gases through three-dimensional polymers depends on two main factors including the penetration rate and solubility. In molecular dimensions, the penetration is a function of the type and the volume of free space in the polymer chains. On the other hand, the solubility in polymers is a

function of the interaction between the penetrating material and the polymer[9,10].

The poly 2-acrylamido- 2- methyl propane sulfonic acid (PAMPS) consists of oxygen and nitrogen groups such as NH, OH, and COOH, as well as the sulfonic acid groups[18]. All of these functional groups are hydrophilic groups that are very powerful making them absorb the water up to 100 times of their initial weight. So, it should be used in cases that require water extraction, such as medicine, drug and agriculture. Also, this polymer can crosslink with different materials and crosslinking plays a very important role in the activity of this membrane material[18]. This polymer is also able to bind to the GO or reduced graphene oxide (rGO) and adding these two materials to the polymer increases its various properties such as barrier properties and electrical properties. Researches have shown that by adding 5wt% of GO to the PAMPS polymer, the membrane's capacity for water absorption increased up to 2 times. Besides, it has a great performance in maintaining this amount of absorbed water. This characteristic results from very high adhesion between water-soluble groups in the polymer and GO and water molecules[18,19].

PAMPS is a brittle polymer with hydrophilic nature. As its density increases, its elasticity and tensile strength decrease so that the structure will be brittle. The presence of the GO solves this problem. Adding the GO reduces fragility. GO acts as a filler in the structure of polymeric membranes because of the presence of hydrophilic functional groups on the GO surface. Nano-sized GO particles could modify the water vapor permeability of composite membranes[20-22].

The addition of the GO makes the PAMPS-GO bonding more elastic, which is resulted from the physical crosslinking mechanism between the polymer and the GO nanosheets. It has been shown that the H-bond interactions between the polymer chains and the GO transfer load between the GO nanosheets and the polymer chains, which increase the mechanical properties.

Additionally, the GO can rotate parallel to the strain axis in the PAMPS lattice during stretching, which leads to the loss of strain[23-25].

The membrane exhibits its hydrophobic properties by adding the GO to the hydrophilic and hydrophobic polymeric compounds, which is due to increased surface roughness. GO incorporation leads to the increase in the contact angle (CA) and improves the roughness of the membrane surface and also increases the porosity. A higher contact angle reflects more hydrophobicity to the membrane surface and increases the membrane porosity. Results of previous researches have shown that the CA is significantly increased by adding the GO into the polymer matrices due to the increase in the membrane porosity and surface roughness. Also, the increase in the porosity caused more folding of GO at the membrane surface[26,27].

Liu et al[12,13] have used an improved PU membrane by adding the GO to investigate its performance for separation of the water from oil in the water/oil system. Interaction of an aminic agent with the GO and then adding this functionalized GO to the PU increased the surface roughness and decreased the surface energy, which ultimately increased the hydrophobic properties of the PU. So, its application is perfectly reasonable for the oil/water separation such that, the oil passes through the membrane and the membrane is not permeable to the water. Their results showed that the amount of water in the oil was very low after passing the membrane, indicating that the PU-GO membrane is not permeable to water and permeable to oil[12,13].

GO has a high surface energy, which is due to the presence of many electrons and can react more easily with the matrices. When it is added to the PU polymer, the electron part enters into the polymer structure and reduces its surface energy. On the other hand, the surface roughness increases, so the polymer becomes hydrophobic. As the surface energy increases, the roughness of the surface decreases and the surface becomes even and smooth, resulting in increased hydrophilicity[28].

Hao et al[29] developed a porous carbon cuboid with a high hydrophilicity comparable to compounds such as MOFs (with high functional groups and rich micro-porosity). Porous carbon cuboids show surface heterogeneity and a high density of narrow micro-spores. These materials, with excellent properties such as fast kinetics and high uptake have been shown to capture water vapor (as polar compound). In these hydrophilic materials, the synergistic effects between micropore structure and surface heterogeneity are greatly enhanced, leading to excellent water capture performance as a polar compound among porous carbon.

Surface functional groups (as polar sites) determined low-pressure water vapor capture capability, which leads to stabilize and induce the dense water phase by the formation of hydrogen bonds. Water vapor capture can be low due to very small number of active sites. Which also prevents from forming hydrogen-bonding network between the water phase and carbon pore walls. Low water vapor capture may be due to the unappropriated micropore sizes, which pre-

vents hydrogen bonds from forming between water vapor molecules. It has been shown that the micropore structure and active sites cause the trapping of water vapor into nanopores. The numerous narrow micropores can also increase the dispersion interactions between the pore walls and the water phase[29].

Hao et al[30] also synthesized bipolar nanocarbon hybrids. The hybridization of the hydrophilicity and hydrophobicity was performed through a coating method. A thin layer of MOF was coated on the surface of nanocarbons. After pyrolysis, nanocarbon hybrids were attained. In this study, a useful procedure was established to prepare hydrophilic nanocarbons with not only surface hydrophilicity of nanocarbons proven by its unique water molecule adsorption but also a micropore size distribution in porous carbons. Their work provided a new insight into how the surface in both organic and aqueous solutions can be expanded by designing bipolar surface structures of nanocarbons with numerous heteroatom-doping.

Nanoporous carbons are necessary materials for development and research as well as for different applications in the scope of separation and adsorption, catalyst supports, energy-storage systems, and so on because of their grand properties such as well-controlled pore structure, highly developed porosity, high stability and conductivity to name only a few. Surface chemistry of porous carbons is much less controllable, because most carbons are dominantly nonpolar showing a hydrophobic surface, although pore structures of porous carbons can be ideally tuned. Nowadays, surface oxidation by dry and wet agents (such as H_2O_2, O_3, nitric acid), N-doping, and plasma treatment are established for producing many polar carbon surfaces[30].

The micropores in the conductive nanocarbons (such as graphene, CNTs) can act as transport shortcuts for the fast transport of electrolyte ions and electrons, achieving an excellent rate efficiency. Because of such surface chemistry and unique structure, the bipolar nanocarbons attain pore volume utilization rate and a higher surface, enhancing the performance of the materials[30].

The present study was carried out to investigate the effect of adding GO on the hydrophilicity, hydrophobicity, and permeability of PAMPS and PU-based membranes against polar materials such as water, ammonia and non-polar materials such as dichloromethane and a mixture of NH_3/CH_2Cl_2 in the vapor phase.

2 Materials and Methods

2.1 Preparation of the samples

2.1.1 GO preparation

GO was prepared using the Hummers´method according to the literature[31,32]. 5 g of graphite powder (Merck, USA), 5 g of $NaNO_3$ (Merck, USA), and 250 mL of H_2SO_2 (98%, Merck, USA) were stirred at 0 to 5 ℃ for 1 h. Then, 5 g of $KMnO_4$ (Merck, USA) as an oxidizing agent was added to the mixture. During the addition of the oxidizing agent, the temperature remained below 20 ℃. The mixture was stirred vigorously for 1 h. In the following, 100 mL of deionized water was added to the mixture after 2 h, and 150 mL of deionized water was added and stirred for 12 min at ambient temperature. Subsequently, 50 mL of H_2O_2/water (1∶1 ratio) was added, and then the resulting solid was separated from the mixture by centrifuging at 4 ℃ with 5 000 r/min. Finally, 40 mL of HCl (5%) was added to the obtained solid. The mixture became clear, and then the solid was washed using water (pH-neutralized). The solid material was separated using a refrigerated centrifuge, at 4 000 r/min. The product was dispersed in the tetrahydrofuran (THF, Merck, USA) as a solvent under ultrasonication for 20 min.

2.1.2 AMPS Polymerization

The 2-acrylamido- 2-methyl propane sulfonic acid (AMPS) was used as a monomer. 10 g of AMPS monomer was dissolved in deionized water, and 0.1 g of potassium sulfate ($K_2S_2O_8$, Merck, USA) was added and stirred in an N_2 atmosphere for 30 min. Then, it was stirred under the N_2 atmosphere at 65 ℃ for 5 h. Finally, the solution was cooled and the resulting gel was placed in an oven for 24 h to obtain a dry polymer[19].

2.1.3 Polyurethane polymerization

Polyurethane (PU, with a grade of 50) was prepared by mixing the polyol and isocyanate. 15 g of polyol (ethylene glycol) was dissolved in the THF (Merck, USA) as a solvent, and then 5 g of isocyanate (3∶1 ratio) was added. The mixture was stirred vigorously for 10 min and placed in a Teflon mold to be dried[12,13].

2.2 Preparation of the membranes

2.2.1 Free-standing GO

Free-standing GO (f-GO) was prepared by the vacuum filtration-assisted method as described in the literature[33] using the filter paper (Rundfilter MN640md, Germany). The GO dispersed in water was directly poured on the filter paper and water was removed by filtration, and then a very thin sheet of the membrane was made. After drying of the film, the filter paper was removed.

2.2.2 PU-GO

PU-GO was a polymer made from a combination of GO and PU. The PU was prepared through the polymerization method described in Section 2.1.3. First, 10 g of polyol was dissolved in the THF and then, 20 wt.% of GO was dispersed in the THF and 5 g of isocyanate under ultrasonication for 20 min. Then, the mixture was added to the polyol mixture and stirred vigorously by a mechanical stirrer for 3 h. Next, the resulting mixture was molded by a casting method[12,13]. These membranes were called PU-20-GO, where the PU polymer contained 20 wt.% of GO in the PU-GO membrane.

2.2.3　PAMPS-GO

PAMPS-GO was the AMPS polymer modified with the GO. As mentioned in Section 2.1.2, AMPS was polymerized, but before final gelation, 20 wt.% of GO was added to the mixture and sonicated for 30 min. The sample was brittle, so 20% *w/w* of dioctylterephthalate (DOTP, SIGMA, USA) was added. The mixture was stirred for 4 h using a mechanical stirrer. Then, the resulting mixture was poured on a filter paper. After drying of the mixture for 24 h at room temperature, the paper was removed. The prepared membrane was called PAMPS-20-GO, where the PAMPS polymer contained 20 wt.% of GO.

2.3　Characterization Methods

XRD (PW3040 Philips with Cu $K\alpha = 1.540\,560$) was used to study the structure of prepared membranes. For this purpose, a comparison was made between standard data (Joint Committee on Powder Diffraction Standards, JCPDS) and the XRD patterns of as-prepared samples. The interlayer spacing was calculated, based on the Braggs´ Equation[34]. Field Emission Scanning Electron Microscopy (FESEM, TSCAN) was used to study the structure of as-prepared membranes. Contact angle test (DSA100 optical contact angle, Germany) was used to investigate the hydrophobicity or hydrophilicity of membrane surfaces. Fourier Transform Infrared Spectroscopy (FT-IR, ALPHA, and Bruker, Germany) was used to identify organic compounds and their functional groups. This method was also used to determine various chemical bonds. The mechanical strength of as-prepared membranes was characterized by a universal mechanical tester (Instron, USA).

The porosity of the membrane samples was computed using the gravimetric procedure. Samples were immersed in isopropyl alcohol (IPA). Then, the wet and dry weight of the samples was measured. The porosity of the membrane samples was obtained based on Equation (1).

$$\varepsilon = \frac{\dfrac{w_2 - w_1}{\rho_i}}{\dfrac{w_2 - w_1}{\rho_i} + \dfrac{w_2}{\rho_P}} \tag{1}$$

Where, w_1 is the dry weight of the sample (g), w_2 represents the wet weight of the sample (g) along with IPA, ρ_i and ρ_P are the densities of IPA (0.79 g/cm^3) and polymer (PU, PAMPS, f-GO (0% polymer). At first, the samples were weighed in the same dimension and then, they were immersed in the IPA at 30 ℃. After 24 h, the residual IPA was removed and the samples were re-weighed. The porosity of the samples was measured using Equation (1)[35].

2.4　Permeability test

For evaluation of the permeability of the membranes, ASTM E96-M14 was used to measure the weight loss of the vessels containing test solutions. According to Fig. 1, during this experiment, a certain amount of the mixture of pure ammonia and dichloromethane (Merck, with a purity of 25 wt.%, and 99%) and deionized water was placed into the sample container and its weight loss was monitored during 144 h (6 days)[21,22].

Weight loss percentage is a good criterion for comparing the ability of membrane permeation, because, in this case, the initial weight of the samples is eliminated. Weight loss percentage of the samples was calculated using the Equation (2)[21,22]:

$$\text{Weight loss} = \frac{(\text{Initial weight} - \text{Final weight})}{(\text{Initial weight})} \times 100 \tag{2}$$

Equation (3) was used to check permeability according to ASTM E96-M14 device. Where, VP, W_1, and W_2 are the vapor permeability, initial weight, and final weight after 6 days, respectively. Also, A is the cross-sectional area of the container (m^2)[21,22].

$$\text{VP} = (W_1 - W_2)/144A \tag{3}$$

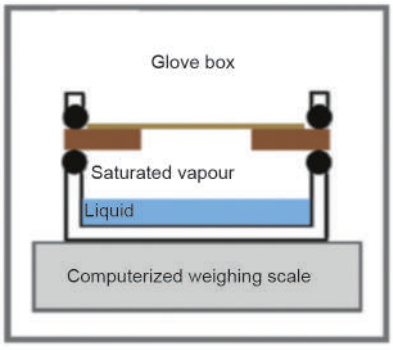

Fig. 1　Schematic of the permeability test[4].

3 Results and discussion

3.1 Characterization

Fig. 2 shows the XRD patterns of all the prepared membrane samples. As shown in Fig. 2, the PAMPS membrane has not a distinct crystalline structure like PU membrane and its structure is amorphous and only a broad peak is observed at 20°, corresponding to the PAMPS structure[22,36]. Based on the calculated results using the Bragg's Equation, the interlayer spacings of PAMPS and PAMPS-20-GO were estimated to be 0.55 and 0.49 nm, respectively.

Only one peak was observed at approximately 11° (JCPDF-75-2078) for f-GO samples (Fig. 2), which was attributed to the GO structure in the samples[31,32]. The interlayer spacing for f-GO was calculated to be about 0.6 nm.

As depicted in Fig. 2, only one broad peak was observed for the PU sample in the range of 10°-28° with a maximum of 19°, corresponding to the PU formation, and the interlayer spacing of this sample was about 0.45 nm, which was similar to the other results[12,13].

As shown in Fig. 2, similar to the PU sample, a wide peak was observed in the XRD pattern for the PU-20-GO membrane in the range of 11° to 28° with a maximum of 19°, corresponding to the formation of PU. No single sharp peak was observed at 11° corresponding to the GO, due to the strong interaction between GO and PU in the membrane structure. This meaned that GO sheets were completely located between the polymer cavities and had no GO adjacent to the polymer surface. As a matter of fact, after adding the GO to the polymer, GO entered into the structure and was not freely observed in the polymer structure[12,13]. However, the calculation showed that the interlayer spacing for the PU-20-GO was about 0.43 nm.

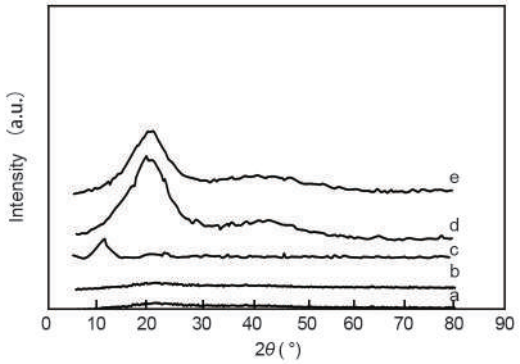

Fig. 2 XRD patterns of samples, (a) PAMPS, (b) PAMPS-20-GO, (c) f-GO, (d) PU and (e) PU-20-GO.

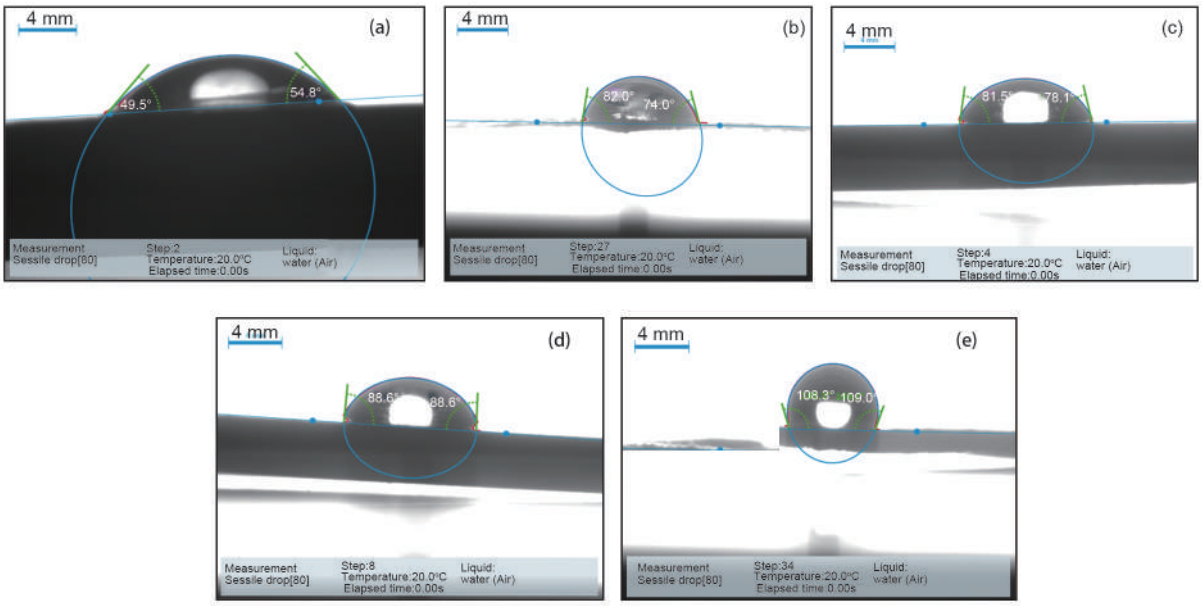

Fig. 3 The contact angle results for (a) f-GO, (b) PAMPS-20-GO, (c) PAMPS, (d) PU and (e) PU-20-GO.

As a qualitative test, the CA test was used to evaluate the hydrophobicity or hydrophilicity of as-prepared membrane surfaces. The lower contact angle of the water droplet in the membrane sample has the higher hydrophilicity, and if the contact angle is higher than 90°, it indicates more hydrophobicity[12,13]. As can be seen in Fig. 3(a), for f-GO samples, the contact angle was less than 90°, indicating its hydrophilicity, which was related to its higher oxidation degree, more oxygen functional groups, and more polarity[37]. The PAMPS and PAMPS-20-GO samples exhibited relatively hydrophilic behavior and their

contact angle was less than 90°. On the other hand, the PU and PU-20-GO samples exhibited hydrophobic behavior and their contact angle was higher than the 90°. The CA of PU-20-GO membrane was greater than the PU membrane. According to the results obtained from the CA test and SEM images, the addition of the GO to the PU increased the surface roughness and decreased the surface energy, which ultimately increased the hydrophobicity of the PU-20-GO, which was consistent with previous researches. Table 1 presents the results of the CA test.

Table 1　The contact angle of the samples.

Samples	Contact angle
f-GO	49.5°-54.8°
PU	88°
PU-20-GO	108°-109°
PAMPS	78°-81°
PAMPS-20-GO	74°-82°

As shown in Fig. 4(a), the f-GO sample had a uniform surface, while the other four samples showed a porous surface. The strength of the bonds between the atoms in the structure of materials was the main reason for the difference between the f-GO sample and the others[4,38,39]. In the first sample (f-GO), due to the low C/O ratio compared to other samples, it seemed that higher adhesion forces between the GO particles on the surface of the membrane led to lower roughness than the other samples. In addition, the results of the CA test also showed that the f-GO sample had a smaller CA than the other samples, which was due to smooth surface and greater bonding energy[4,38,39].

As depicted in Fig. 4(b), the PU sample showed a relatively uniform and unwrinkled surface compared to Fig. 4(c) (PU-20-GO sample), where the surface of the membrane had uniform folds, indicating the presence of GO at the structure. An important point in this sample was that these wrinkles increased the surface roughness and thus increased the hydrophobicity of this sample.

The PAMPS sample, shown in supplemetary, exhibited a perfectly flat surface without any folding. This will increase the surface energy and make the sample hydrophilic. As can be seen in Fig. 4(d), the PAMPS-20-GO sample showed an unwrinkled surface, which reduced the surface energy and increased the surface roughness compared to the f-GO sample. This roughness was lower in the PAMPS-20-GO sample than the PU samples, and its surface was more uniform than the PU samples. However, the PAMPS polymer is smooth, brittle, and non-porous, and the addition of the GO would decrease its brittleness[18,19].

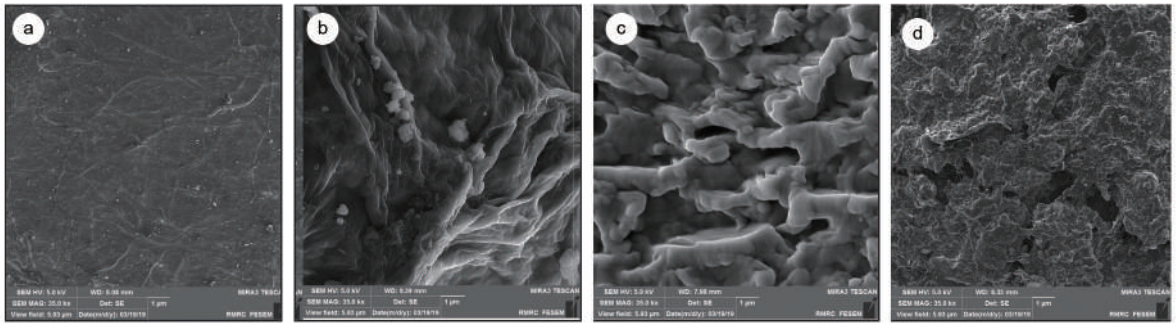

Fig. 4　FESEM micrographs of the membrane samples: (a) f-GO, (b) PU, (c) PU-20-GO and (d) PAMPS-20-GO.

Figs. 5 and 6 show the results obtained from the FT-IR test. For the f-GO sample, the peaks were observed at 3 607, 1 728, 1 622, 1 443, and 1 041 cm^{-1}, corresponding to the presence of hydroxyl, carbonyl, C－OH, and epoxide groups, respectively[5]. In the PU polymer without GO, the peaks observed at 3 590, 2 840, 2 377 and 1 742 cm^{-1} correspond to NH, CH, NCO, and C═O (amide) bonds, respectively[12,13]. For the PU-20-GO sample, the peak at 3 445 cm^{-1} corresponds to of NH and OH bonds, other peaks at 2 354 and 2 970 cm^{-1} are related to CH and NCO links between PU and GO[12,13].

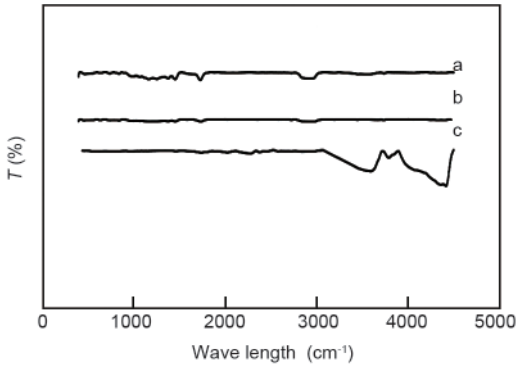

Fig. 5　FT-IR of samples: (a) f-GO, (b) PU-20-GO and (c) PU.

Fig. 6 shows the results of the FT-IR test for PAMPS samples with and without GO. The peaks at 1 610, 1 364, 1 241, 1 543 and 3 500 cm^{-1} are vinyl bond, S = O, NH, and OH groups, respectively. In the PAMPS-20-GO sample, the peak at 1610 cm^{-1} is related to the vinyl bond, and the peaks at 1 364 and 1 241 cm^{-1} are related to S = O, the peak at 1 547 cm^{-1} is attributed to NH, the peak at 3 305 cm^{-1} is related to OH, the peak at 1 031 cm^{-1} is related to the alkoxide and finally, the peak at 1 724 cm^{-1} is related to C = O[19]. Supplementary data are also provided presenting the results of each test individually.

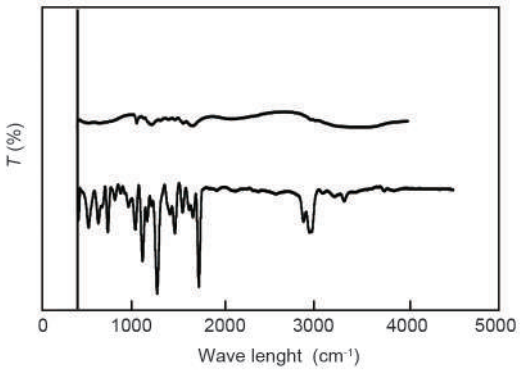

Fig. 6 FT-IR patterns for (a) PAMPS and (b) PAMPS-20-GO.

Table 2 shows Young's Modulus for all the samples. According to Table 2, Young's Modulus (MPa) increased by adding the GO in the PU and PAMPS structures. This may be due to the interaction between the NH bond in the polymer matrix and oxygen functional groups in the GO, which resulted in hydrogen bonding[2]. In PAMPS and PAMPS-20-GO samples, the structure of the PAMPS -based membrane was glassy but the PAMPS-20-GO sample showed an elastic nature. Accordingly, the elasticity of PAMPS polymer was increased by adding the GO.

Table 2 Young's Modulus of prepared membrane samples.

Membrane code	Young's Modulus
f-GO	68.3 GPa
PU	58 MPa
PU-20-GO	122 MPa
PAMPS	75 MPa
PAMPS-20-GO	105 MPa

Assembly of 2D GO sheets into the 3D polymer network has attracted a remarkable interest owing to their unique structures and excellent properties[40]. Results of a previous study showed that the addition of the GO resulted in the excellent structural property in the GO/polymer composite in terms of pore size and porosity[35]. The addition of hydrophilic materials such as GO and rGO into the polymer membranes resulted in modified membrane performance. Especially, physical and structural enhancement of the polymer by the GO resulted in increased porosity and hydrophilicity, which significantly improved the performance of the polymer membranes. Hydrophilicity, porosity and pore size of the polymer membranes are the quantitative parameters that were influenced by the GO[35].

According to the SEM images, the f-GO membrane had a smooth surface without folding. Its porosity was 3% as shown in Table 3, indicating a smooth surface without a high surface energy. Therefore, it had hydrophilic behavior as confirmed in the CA test. The PAMPS membrane sample had a porosity of about 10%, indicating that it had less hydrophilic behavior than the f-GO membrane. According to the SEM images, the PU membrane had a porous surface and wrinkle was observed on the surface of the membrane, and its porosity was about 31%. It had a lower surface energy than the previous two samples, so it exhibited hydrophobic behavior. The results of the porosity test were consistent with those of the CA test. The PAMPS- GO membrane had a higher porosity than the PAMPS membrane. However, it had less surface energy than the PAMPS membrane and had higher surface energy than the PU membrane, which was similar to the results of the CA test. The PU -GO membrane had a more porous surface than the other samples and its porosity was about 42%.

Table 3 Porosity for prepared membrane samples

Samples	Porosity (%)
f-GO	3
PU	31
PU-20-GO	42
PAMPS-20-GO	13
PAMPS	10

3.2 Permeability test

Fig. 7 shows the permeability of all the membranes against ammonia solution for 144 h. These results were presented in terms of weight loss percentage calculated using the Eq. (1).

According to the results of Fig. 7, the largest drop in weight was found for the f-GO sample. On the other hand, the PU-20-GO sample had the lowest weight loss at the end of test, which was due to a higher interlayer spacing of f-GO, its higher amounts of oxygen functional groups, and a lower C/O ratio, favorable for absorbing ammonia[41,42].

It seemed that the negative charge and pores in the structure of the polymer membrane were increased

by the addition of GO into the PU, which prevented the diffusion of ammonia vapors through the membrane. Because of the high electronegativity of nitrogen than the hydrogen in the ammonia structure, hydrogen atoms will have a relatively positive charge, resulting in a high negative charge in the membrane structure due to the presence of oxygenated functional groups in the GO. Also, because of the long penetration pathway in the membrane and increased porosity, ammonia molecule was attached to the GO and remained in the diffusion pathway, which led to its low penetration (the size of the ammonia molecule was equal to 0.326 nm). Lower C/O ratio and higher surface charge of the PU-20-GO sample led to greater oxygenated functional groups and increased porosity compared to the other samples and this membrane acted as a barrier against permeation of ammonia[41,42].

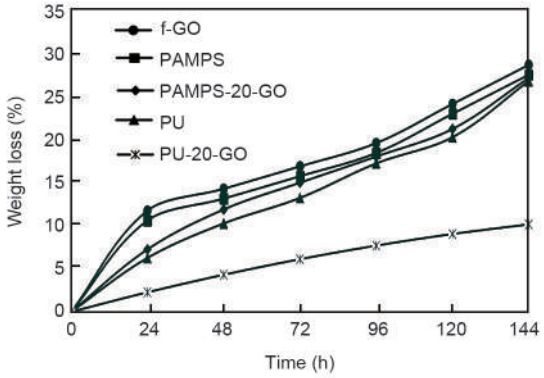

Fig. 7　Weight loss percentage of ammonia for all samples.

In the ammonia structure, the N atoms have a negative charge and H atoms have a positive charge, which is due to the higher electronegativity of nitrogen than the hydrogen. However, the charge of the PU-20-GO membrane structure was negative due to the presence of oxygenated functional groups in the GO. On the other hand, the long penetration pathway created in the membrane due to increased porosity led to the absorption of ammonia molecule and lowered weight loss (the size of the ammonia molecule was about 0.326 nm)[41,42].

The higher tendency of ammonia to be absorbed by GO was observed due to the presence of oxygen functional groups and high surface charge, which was due to the presence of more oxygen-containing functional groups in the f-GO sample. As shown in Fig. 8, the lowest vapor pressure (VP) in the samples was found for the PU-20-GO sample, which was similar to the results of weight loss (Fig. 7). Again, high surface charge in the PU-20-GO sample and increased porosity compared to the other samples led to decreased permeability of ammonia vapors.

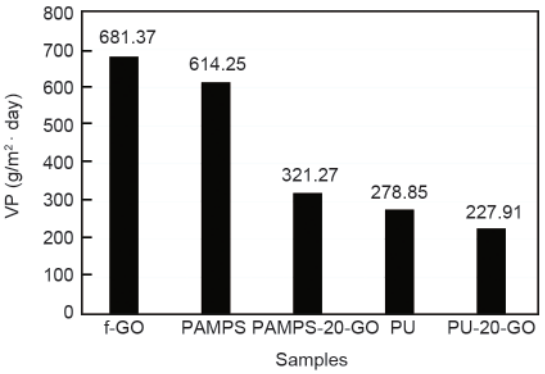

Fig. 8　VP of all samples for ammonia.

As depicted in Fig. 8, the highest weight loss occurred in the PAMPS-20-GO and PAMPS membranes due to the presence of GO large negative charges in the PAMPS membrane. However, the PAMPS is an anionic polymer[36] and it seems that synergistic effects of negative charges of polymer and GO led to the low interaction between these two materials, so there was a negligible effect on the rate of ammonia permeation through these membranes.

Fig. 9 shows the permeability results of all the membranes against dichloromethane. These results were presented in terms of the weight loss percentage based on the Eq. (1).

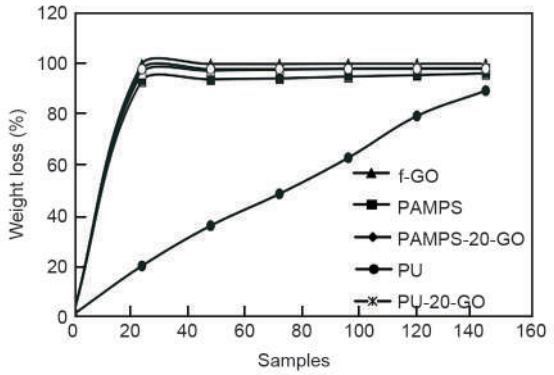

Fig. 9　Weight loss percentage of dichloromethane for all samples.

According to the results shown in Fig. 9, except for the PU membrane, the permeability of dichloromethane, as a non-polar material through the other membranes was very high, such that even more than 96% of solvent passed through these membranes. The PU-20-GO and GO samples showed the maximum weight loss, which was due to the presence of negative charge in the structure of the membranes resulted from the presence of oxygen-containing functional groups and the high selectivity for CH_2Cl_2 in the membrane samples except for the PU membrane. As noted earlier, the addition of the GO into the polymer increased the negative charge and porosity of the

structure in the polymer membrane that favored for passage of dichloromethane vapors and their penetration through the membrane. Due to the high electronegativity of chlorine relative to carbon in the structure of dichloromethane, chlorine atoms will have a slight negative charge. So, as a result of a high negative load in the membrane structure, which was due to the presence of GO oxygenated groups, the dichloromethane molecule had not been absorbed. Also, the presence of a three-dimensional polymer structure and a two-dimensional filler of GO led to the high selectivity of polymer membranes for dichloromethane, indicating that all the polymer membranes except for the PU membrane had a very high permeable for dichloromethane[9,10,43]. So, most of the dichloromethane was evaporated and passed through all free-standing membranes (except PU) after about 96 h.

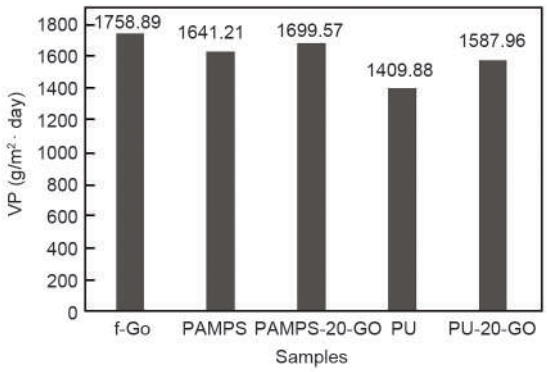

Fig. 10 VP of all samples for dichloromethane.

As shown in Fig. 10, the lowest VP in the GO samples was found for the PU sample, and the highest VP was found for the f-GO sample. However, all the membranes showed much higher dichloromethane permeation compared to ammonia permeation, confirming the high tendency of the membrane for the absorption of dichloromethane. PU sample had only the three-dimensional polymer structure in the membranes that did not have any filler. This is why it showed a lower tendency for the absorption of dichloromethane than other samples with GO.

The NH_3/CH_2Cl_2 mixture was prepared to assess the permeability of polar/non-polar materials. Fig. 11 shows the permeability results of all the membranes against the NH_3/CH_2Cl_2 mixture.

For the ammonia-dichloromethane mixture, as the boiling points of these two solvents are close 37 and 39 ℃, respectively. the two solvents were evaporated consequently, and ammonia concentration in vapor phase was higher than dichloromethane because of its higher volatility. After the passage of this mixture through the membranes, ammonia was adsorbed by the oxygenated groups in the GO and dichloromethane was eliminated due to the relatively positive charge of the hydrogen atoms in the ammonia structure and the negative charge on the chlorine atoms in dichloromethane. Subsequently, the pathway through the layers was blocked by the ammonia molecule, thus the permeation rate of dichloromethane reduced during the test time. Besides, three-dimensional polymer membranes with two-dimensional GO fillers were impermeable to ammonia. However, the absorption of a high amount of ammonia vapors in the penetration pathway led to the blockage of the porosities in the membrane structure. However, based on the experimental results, all of the dichloromethane passed through the membranes and 90% of ammonia remained in the test cup.

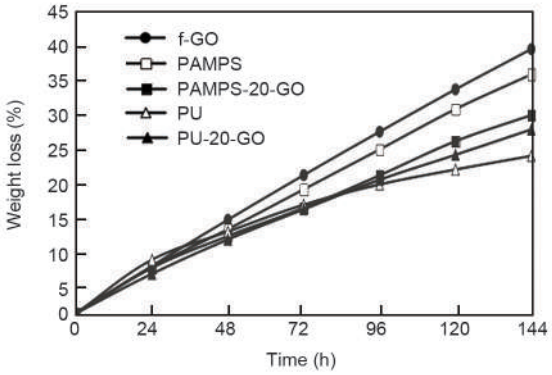

Fig. 11 Weight loss percentage of all samples for the ammonia-dichloromethane mixture.

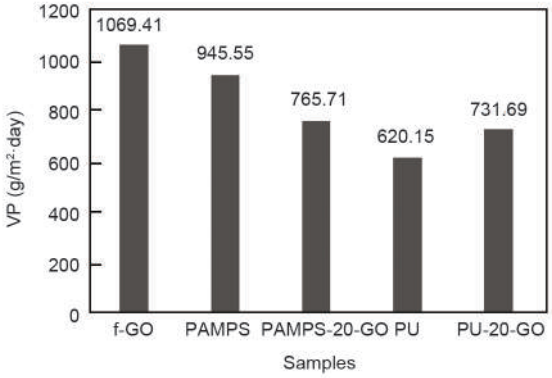

Fig. 12 VP of all samples for the NH_3/CH_2Cl_2 mixture.

As shown in Fig. 12, the maximum and minimum vapor permeation were found for the f-GO and PU membranes, respectively. However, the f-GO sample had a higher interlayer spacing and a lower negative charge in its structure. For the PAMPS sample, a higher interlayer spacing than the other polymer samples led to a higher VP in the polymer samples. For the PAMPS-20-GO sample, its higher hydrophilicity compared to the other polymer samples, as well as its greater interlayer spacing compared to the PU

and PU-20-GO polymer samples resulted in a higher VP compared to the membrane samples.

Fig. 13 presents the results of the water vapor permeability test for all the membranes. These results were presented in terms of the weight loss percentage calculated by Eq. (1).

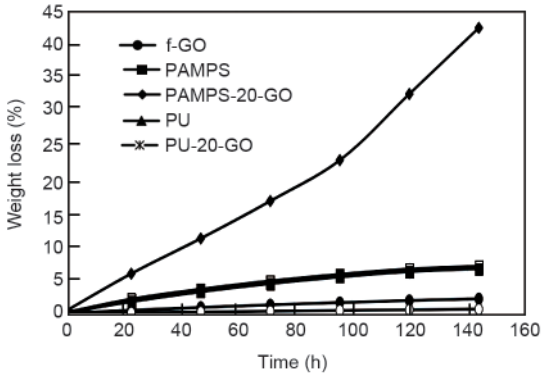

Fig. 13　Weight loss percentage of all samples for water.

As noted earlier, the negative charge and porosity of the structure in the polymeric membranes were increased by adding GO into the PU and PAMPS polymers that led to inhibition of the water vapor permeation through the related membranes. Because of a higher electronegativity of oxygen in comparison with hydrogen, in the water structure hydrogen atoms will have a positive charge, resulting in a high negative charge in the membrane structure. On the other hand, the presence of oxygen functional groups in the GO and alsoa long pathway through the membrane resulted from increased porosity led to the absorption of water molecules by the GO. Consequently, these absorbed molecules remained in the structure and blocked the penetration pathways. It should be noted that the size of the H_2O molecule was about 0.275 nm, therefore the blockage occurred in the pathways in the membranes.

The PU-GO membrane is fully porous, so positive-charge water molecules (due to the presence of hydrogen atoms) were adsorbed to the membrane and were not allowed to pass through the membrane due to high porosity and negative charge in the membrane structure. The PAMPS-GO polymer membrane behaved similarly to the PU-GO membrane because PAMPS is an anionic polymer[36,44,45].

As depicted in Fig. 13, the lowest weight loss was found for the PU-20-GO sample (0.63%), which was attributed to a lower C/O ratio in the GO that caused a higher negative charge and prevented water from infiltration. It should be noted that the PU (with a grade of 50) was used as an inherently waterproof polymer, so the hydrophobic behavior was quite natural in all the related membranes[8,11-13].

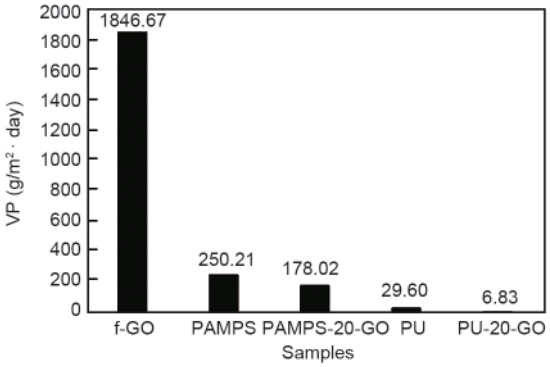

Fig. 14　VP of all samples for water.

As shown in Fig. 14, the lowest VP in the samples was found for the PU-20-GO sample and the highest for the f-GO sample. Lower hydrophilicity and high surface charge in the PU-20-GO sample led to a higher proportion of oxygenated particles and increased porosity, which was due to the presence of GO filler. This is why the PU-20-GO membrane acted as a barrier towards water. The PAMPS-20-GO sample showed a higher permeability towards water than PU membranes.

The f-GO membrane had a very negative electric charge. On the other hand, hydrogen atoms have a positive charge in the water and ammonia, because of higher electronegativity of oxygen and nitrogen than hydrogen. Therefore, they were absorbed into the f-GO membrane by forming van der Waals forces or the electrostatic interaction between these molecules and the f-GO membrane. However, PU-GO and PAMPS-GO membranes had a less negative charge, so they had less water and ammonia absorption than f-GO membranes. For dichloromethane, it had a high permeability into all the membranes due to its negative charge nature[46].

4　Conclusions

PU and PAMPS polymers as the membranes were compared both individually and composited with 20 wt.% of GO. The effect of polymer structure and hydrophilicity or hydrophobicity on the permeability of the membrane was studied. The results of the XRD analysis showed that PAMPS samples had an amorphous structure, and the main peak in the PU samples was attributed to the presence of PU without the peak for GO because of the good dispersion of GO. The results of the FESEM test showed that the roughness, porosity, and folding of the membranes were increased by adding 20 wt.% of GO into the PU or PAMPS polymers, but the GO -containing PAMPS

samples showed lower roughness than the GO-containing PU samples. The roughness and folding results were verified by the contact angle test. Permeability of the membranes was evaluated against ammonia and water as polar molecules and also dichloromethane as a non-polar molecule. The results showed that adding the GO to PU or PAMPS polymers can increase the negative charge and the interlayer spacing. The presence of this negative charge increased the amount of absorption of polar species. For nonpolar species, these membranes were highly permeable. Therefore, the composites had high selectivity for the ammonia-dichloromethane.

References

[1] Lee C T, Y S Wang. High-performance room temperature NH_3 gas sensors based on polyaniline-reduced graphene oxide nanocomposite sensitive membrane[J]. Journal of Alloys and Compounds, 2019, 789: 693-696.

[2] Smith A T, A M LaChance, S Zeng, et al. Synthesis, properties, and applications of graphene oxide/reduced graphene oxide and their nanocomposites[J]. Nano Materials Science, 2019, 1(1): 31-47.

[3] Lee S P, G A Ali, H Algarni, et al. Flake size-dependent adsorption of graphene oxide aerogel[J]. Journal of Molecular Liquids, 2019, 277: 175-180.

[4] Ma J, D Ping, X Dong. Recent developments of graphene oxide-based membranes: a review[J]. Membranes, 2017, 7(3): 52.

[5] Huang H, Y Mao, Y Ying, et al. Salt concentration, pH and pressure controlled separation of small molecules through lamellar graphene oxide membranes[J]. Chemical Communications, 2013, 49(53): 5963-5965.

[6] Kim H W, H W Yoon, S M Yoon, et al. Selective gas transport through few-layered graphene and graphene oxide membranes[J]. Science, 2013, 342(6154): 91-95.

[7] Shen J, M Zhang, G Liu, et al. Facile tailoring of the two-dimensional graphene oxide channels for gas separation[J]. RSC advances, 2016, 6(59): 54281-54285.

[8] Song W, B Wang, L Fan, et al. Graphene oxide/waterborne polyurethane composites for fine pattern fabrication and ultrastrong ultraviolet protection cotton fabric via screen printing[J]. Applied Surface Science, 2019, 463: 403-411.

[9] Noh M J, M J Oh, J H Choi, et al. Layer-by-layer assembled multilayers of charged polyurethane and graphene oxide platelets for flexible and stretchable gas barrier films[J]. Soft Matter, 2018, 14(32): 6708-6715.

[10] Kim D W, H Kim, M L Jin, et al. Impermeable gas barrier coating by facilitated diffusion of ethylenediamine through graphene oxide liquid crystals[J]. Carbon, 2019, 149: 28-35.

[11] Zhang Y, J Ma, Y Bai, et al. The preparation and properties of nanocomposite from bio-based polyurethane and graphene oxide for gas separation[J]. Nanomaterials, 2019, 9(1): 15.

[12] Liu H D, Z Y Liu, M B Yang, et al. Surperhydrophobic polyurethane foam modified by graphene oxide[J]. Journal of Applied Polymer Science, 2013, 130(5): 3530-3536.

[13] Liu Y, J Ma, T Wu, et al. Cost-effective reduced graphene oxide-coated polyurethane sponge as a highly efficient and reusable oil-absorbent[J]. ACS Applied Materials & Interfaces, 2013, 5(20): 10018-10026.

[14] Yang S, L Chen, C Wang, et al. Surface roughness induced superhydrophobicity of graphene foam for oil-water separation[J]. Journal of Colloid and Interface Science, 2017, 508: 254-262.

[15] Zhu H, D Chen, W An, et al. A robust and cost-effective superhydrophobic graphene foam for efficient oil and organic solvent recovery[J]. Small, 2015, 11(39): 5222-5229.

[16] Zhang L, H Li, X Lai, et al. Thiolated graphene-based superhydrophobic sponges for oil-water separation[J]. Chemical Engineering Journal, 2017, 316: 736-743.

[17] Song S, H Yang, C Su, et al. Ultrasonic-microwave assisted synthesis of stable reduced graphene oxide modified melamine foam with superhydrophobicity and high oil adsorption capacities[J]. Chemical Engineering Journal, 2016, 306: 504-511.

[18] Tang Y, C Guan, Y Liu, et al. Preparation and absorption studies of poly (acrylic acid-co-2-acrylamide-2-methyl-1-propane sulfonic acid)/graphene oxide superabsorbent composite[J]. Polymer Bulletin, 2019, 76(3): 1383-1399.

[19] Liu Y, J Li, X Cheng, et al. Self-assembled antibacterial coating by N-halamine polyelectrolytes on a cellulose substrate[J]. Journal of Materials Chemistry B, 2015, 3(7): 1446-1454.

[20] Hemmati K, R Sahraei, M Ghaemy. Synthesis and characterization of a novel magnetic molecularly imprinted polymer with incorporated graphene oxide for drug delivery[J]. Polymer, 2016, 101: 257-268.

[21] Gorji M, A Sadeghian Maryan. Breathable-windproof membrane via simultaneous electrospinning of PU and P (AMPS-GO) hybrid nanofiber: Modeling and optimization with response surface methodology[J]. Journal of Industrial Textiles, 2018, 47(7): 1645-1663.

[22] Gorji M, M Karimi, S Nasheroahkam. Electrospun PU/P (AMPS-GO) nanofibrous membrane with dual-mode hydrophobic-hydrophilic properties for protective clothing applications[J]. Journal of Industrial Textiles, 2018, 47(6): 1166-1184.

[23] Yang C, Z Liu, C Chen, et al. Reduced graphene oxide-containing smart hydrogels with excellent electro-response and mechanical properties for soft actuators[J]. ACS applied materials & interfaces, 2017, 9(18): 15758-15767.

[24] Lian C, Z Lin, T Wang, et al. Self-reinforcement of PNIPAm-Laponite nanocomposite gels investigated by atom force microscopy nanoindentation[J]. Macromolecules, 2012, 45(17): 7220-7227.

[25] Fan J, Z Shi, M Lian, et al. Mechanically strong graphene oxide/sodium alginate/polyacrylamide nanocomposite hydrogel with improved dye adsorption capacity[J]. Journal of Materials Chemistry A, 2013, 1(25): 7433-7443.

[26] Zinadini S, A A Zinatizadeh, M Rahimi, et al. Preparation of a novel antifouling mixed matrix PES membrane by embedding graphene oxide nanoplates[J]. Journal of Membrane Science, 2014, 453: 292-301.

[27] Lindfors T, Z A Boeva, R M Latonen. Electrochemical synthesis of poly (3, 4-ethylenedioxythiophene) in aqueous dispersion of high porosity reduced graphene oxide[J]. RSC advances,

2014, 4(48): 25279-25286.

[28] Xia C, Y Li, T Fei, et al. Facile one-pot synthesis of superhydrophobic reduced graphene oxide-coated polyurethane sponge at the presence of ethanol for oil-water separation[J]. Chemical Engineering Journal, 2018, 345: 648-658.

[29] Hao G P, G Mondin, Z Zheng, et al. Unusual ultra-hydrophilic, porous carbon cuboids for atmospheric-water capture[J]. Angewandte Chemie International Edition, 2015, 54(6): 1941-1945.

[30] Hao G P, Q Zhang, M Sin, et al. Design of hierarchically porous carbons with interlinked hydrophilic and hydrophobic surface and their capacitive behavior[J]. Chemistry of Materials, 2016, 28(23): 8715-8725.

[31] Guerrero-Contreras J, F Caballero-Briones. Graphene oxide powders with different oxidation degree, prepared by synthesis variations of the Hummers method[J]. Materials Chemistry and Physics, 2015, 153: 209-220.

[32] Paulchamy B, G Arthi, B Lignesh. A simple approach to stepwise synthesis of graphene oxide nanomaterial[J]. J Nanomed Nanotechnol, 2015, 6(1): 1.

[33] Romanos G, L Pastrana-Martínez, T Tsoufis, et al. A facile approach for the development of fine-tuned self-standing graphene oxide membranes and their gas and vapor separation performance[J]. Journal of Membrane Science, 2015, 493: 734-747.

[34] Niemantsverdriet J W. Spectroscopy in catalysis: an introduction[Z]. 2007: John Wiley & Sons.

[35] Park M J, S Phuntsho, T He, et al. Graphene oxide incorporated polysulfone substrate for the fabrication of flat-sheet thin-film composite forward osmosis membranes[J]. Journal of Membrane Science, 2015, 493: 496-507.

[36] Cui C, S Zhang. Synthesis, characterization and performance evaluation of the environmentally benign scale inhibitor IA/AMPS copolymer[J]. New Journal of Chemistry, 2019, 43: 9472-9482.

[37] Ramazani S, M Karimi. Electrospinning of poly(ε-caprolactone) solutions containing graphene oxide: Effects of graphene oxide content and oxidation level[J]. Polymer Composites, 2016, 37(1): 131-140.

[38] Tang Y P, D R Paul, T S Chung. Free-standing graphene oxide thin films assembled by a pressurized ultrafiltration method for dehydration of ethanol[J]. Journal of Membrane Science, 2014, 458: 199-208.

[39] Liu H, H Wang, X Zhang. Facile fabrication of freestanding ultrathin reduced graphene oxide membranes for water purification[J]. Advanced Materials, 2015, 27(2): 249-254.

[40] Qiang F, L L Hu, L X Gong, et al. Facile synthesis of superhydrophobic, electrically conductive and mechanically flexible functionalized graphene nanoribbon/polyurethane sponge for efficient oil/water separation at static and dynamic states[J]. Chemical Engineering Journal, 2018, 334: 2154-2166.

[41] Tabr F A, F Salehiravesh, H Adelnia, et al. High sensitivity ammonia detection using metal nanoparticles decorated on graphene macroporous frameworks/polyaniline hybrid[J]. Talanta, 2019, 197: 457-464.

[42] Hu N, Z Yang, Y Wang, et al. Ultrafast and sensitive room temperature NH3 gas sensors based on chemically reduced graphene oxide[J]. Nanotechnology, 2013, 25(2): 025502.

[43] Sun S, S Tang, X Chang, et al. A bifunctional melamine sponge decorated with silver-reduced graphene oxide nanocomposite for oil-water separation and antibacterial applications[J]. Applied Surface Science, 2019, 473: 1049-1061.

[44] An X, H Ma, B Liu, et al. Graphene oxide reinforced polylactic acid/polyurethane antibacterial composites[J]. Journal of Nanomaterials, 2013, 2013(18): 1-7.

[45] Jung K H, B Pourdeyhimi, X Zhang. Synthesis and characterization of polymer-filled nonwoven membranes[J]. Journal of Applied Polymer Science, 2011, 119(5): 2568-2575.

[46] Jia T, S Shen, L Xiao, et al. Constructing multilayered membranes with layer-by-layer self-assembly technique based on graphene oxide for anhydrous proton exchange membranes[J]. European Polymer Journal, 2020, 122: 109362.